CONF-9505173--1

LA-UR-95-121

Title: FORTE Antenna Element and Release Mechanism Design

Author(s): Thomas A. Butler, ESA-EA

David J. Rohweller

Submitted to: Aerospace Mechanisms Symposia
NASA Johnson Space Center
May 17, 18, and 19, 1995

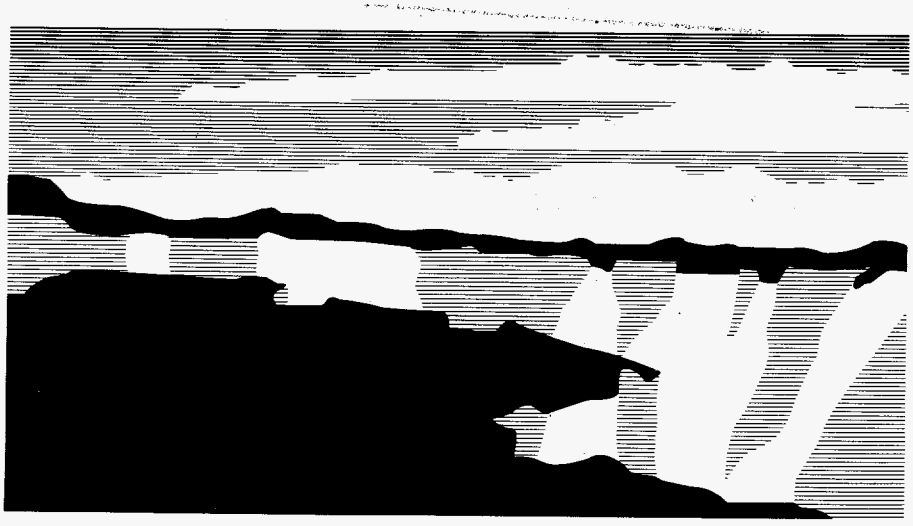

Los Alamos
NATIONAL LABORATORY

FORTÉ Antenna Element and Release Mechanism Design

David J. Rohweller* and Thomas A. Butler**

Abstract

The Fast On-Orbit Recording of Transient Events (FORTÉ) satellite being built by Los Alamos National Laboratory (LANL) and Sandia National Laboratories (SNL) has as its most prominent feature a large deployable (11 m by 5 m) log periodic antenna to monitor emissions from electrical storms on the Earth. This paper describes the antenna and the design for the long elements and explains the dynamics of their deployment and the damping system employed. It also describes the unique paraffin-actuated reusable tie-down and release mechanism employed in the system.

Introduction

The antenna for the FORTÉ satellite for LANL/SNL is a log periodic antenna for detecting broadband electromagnetic pulses associated with natural and man-made events. The antenna elements are stowed for launch within and wound around a concentric stack of rings that separate one at a time as deployment proceeds. As each ring separates, four antenna elements are uncovered and whip out rotationally from the wrap position into the straight position. Extended, the antenna configuration is an array of four 10-element dipole antennas, orthogonal to each other as shown in Figure 1. Each antenna is held in position by a torsion spring that holds the root of the antenna against a stop.

The antenna uses an Astromast™ from Astro Aerospace Corporation to deploy the antenna and support it on orbit. The most challenging design problems were as follows:

1. To design antenna elements that assume a straight position after many months stored in a tight coil, and measure the straightness of the thin elements unaffected by gravity.

2. Analyze the whipping motion of the deploying antenna elements and damp the energy released from the antenna elements so that they are not damaged as they deploy.

3. Develop a reusable release mechanism to release the 4400 N (1000 lb) preload required for launch.

Antenna Element Design

The antenna elements vary in length from 2.45 m (96 in) to 0.55 m (21.5 in) and, when extended, must lie at 20 ±2 degrees above the base plane and at 90 ±2 degrees to each other. These criteria translate to the straightness requirement shown in Figure 2.

For the long thin elements, this straightness is difficult to measure. Additionally, the elements must be capable of coiling onto a 291 mm (11.46 in) diameter cylinder without

*Astro Aerospace Corporation, Carpinteria, CA
**Los Alamos National Laboratory, Los Alamos, NM

taking any permanent set. The following materials were initially investigated to find a high strain capable antenna element:

- Electrodeposited copper on fiberglass rods
- Electrodeposited silver on fiberglass rods
- Copper wire inside a fiberglass pultrusion
- Pultruded graphite epoxy rods

All of these were rejected except the graphite epoxy rods. The original design used graphite rods, 2.54 mm (0.1 in) in diameter. Graphite has the required stiffness, strength, and conductivity to perform as antennas and coil to the required diameter. However, creep tests showed that the elements took a permanent set after storage on the cylinder. The set was slight, but the straightness of the rods is sensitive to slight amounts of creep within the material. This creep translates directly to bow deflection in the rod. The amount of bow deflection allowed on a 2.45 M rod is 21 mm (0.84 in) in a weightless environment. Figure 2 shows the straightness required as the rods get longer in order to stay within the ±2 degree angle.

Several methods for measuring the bow were attempted. The thin rods were deflected 3 mm or so by every measurement system tried, however. One method involved supporting the rods on floats on a water table and measuring the deflection in the horizontal plane to minimize the effect of gravity. The rod tended to sag between the supports, so it was difficult to tell if the maximum plane of bow was parallel to the ground. Also, the results were not repeatable. This method nevertheless demonstrated that the graphite elements did not meet the straightness requirement.

Consequently, titanium spring wire Ti-3Al-8V-6Cr-4Mo-4Zr per AMS 4957 (modified) was tried. It has high strength and a stiffness between that of graphite and fiberglass rods and will not creep significantly in the stowed condition. The diameter was reduced from 2.54 mm to 1.52 mm (0.06 in) to reduce the stowed strain.

A new method was used to measure the straightness of the titanium wire. The wire was hung vertically and the plane of bow was oriented perpendicular to the axis of a jig transit placed 5 m (16 ft) to one side of the wire as shown in Figure 3. The bottom end of the wire was placed in a cup of water to quickly damp its motion (tape flags on the end also helped). The deflection was then measured from the bottom to the center and top of the wire, and the bow in the free state calculated according to the following equation from Timoshenko (ref. 1):

$$b = y\left[1+\frac{TL^2}{\pi^2 EI}\right] \qquad (1)$$

Where:
- b = maximum deflection in free state
- y = deflection under tension
- E = modulus of elasticity
- I = moment of inertia
- T = tension load
- L = length of member

This equation assumes that the wire is weightless, tension is applied to the ends, and that the wire has an initial deflection in the free state. For this calculation, half the weight of the wire was used as the T (tension) value in the equation. This approximation was verified by finite element analysis rather than by deriving the exact equation.

Results of Design and Testing of the Antenna Element

A piece of titanium wire 2.9 m (114 in) long had a measured bow deflection after storage on a cylinder for 3 days of 7.3 mm (0.287 in). This wire was then laid on floats on the water table for 24 hours to allow it to recover without influence. The bow deflection then measured 4.1 mm (0.162 in). This met the requirements of the specification for the longest antenna element, and since the shorter elements have more tolerance, the straightness is acceptable. For margin in meeting the specification, the longest antenna elements were set at 1 degree beyond nominal as shown in Figure 2, since the wire will take a set in only one direction.

Analysis of the Antenna Elements

Mechanics of the Antenna Element Deployment

Two primary concerns exist when the antenna elements are released from the rings around which they are wrapped in the stowed configuration. The first concern is related to the stress in the element at different times during the release sequence. When the element root has moved approximately 90 degrees, it contacts a stop that prevents further rotation of the arm at the root. Thus the base of the element becomes a "fixed" beam with high initial velocity. As the element continues its motion, the stress at the root builds up to high levels. Stress also occurs in the element when the initial planar motion is forced into out-of-plane motion as the arm at the root starts to rotate. The inertia in the moving element resists motion that the arm is trying to enforce. The second concern is that the out-of-plane motion of the antenna may become excessive and allow the longest elements to strike the spacecraft.

Stress in the Element

A simple planar model is sufficient to show that the stress in the element may exceed yield when the arm at the root contacts the stop. It is first assumed that all of the stored potential energy in the element (in the stowed configuration) is transformed into rotational kinetic energy just before the stop is contacted. Using this velocity profile for the initial conditions (when it comes to a stop at the root) shows that the yield stress for titanium is exceeded.

When these calculations were performed for the graphite epoxy antenna elements, it was determined that for planar motion the ultimate stress would be exceeded and the elements would be expected to fracture. The expected stress for this simplified model is independent of element length so it was convenient to verify the validity of the model by testing a deployment of the shortest element set. The test was performed in a vacuum chamber to eliminate the significant effects of air drag on the element after its release.

Results of the test were that the elements were not visibly damaged. Review of high-speed videos of the deployment showed that damage to the elements did not occur for several reasons. First, the motion of the element was not entirely planar. Significant energy is coupled into out-of-plane motion of the element. Also, because of the uncontrolled release of the elements from the canister, higher frequency short wavelength vibration modes in the elements are excited. Some of the original energy is retained in the deformation described by these modes. Finally, the assumption that the arm at the root of the element contacts a rigid stop is not completely valid. The stop and the area of the canister surrounding it have significant local compliance.

Antenna Motion

Review of the high-speed videos shows that out-of-plane motion of the antenna elements is large and may be critical since the longer elements can contact the satellite. This out-of-plane motion is caused by the 20-degree rotation of the arm at the element root, as each element rotates into its final 80-degree angle relative to the mast axis.

Modeling Antenna Deployment

Review of video from the tests led to the conclusion that a better model of the antenna had to be developed for accurately predicting its motion and associated stresses. The finite element (FE) computer code ABAQUS (ref. 2) was chosen for developing the model. ABAQUS is a nonlinear FE code that can easily handle the large motions and other nonlinearities associated with antenna deployment.

A single antenna element was modeled with 16 second-order beam finite elements. The antenna mast was modeled as a rigid cylindrical surface that the element could not penetrate as it deployed. This representation of the mast is important because the element unfurls and then wraps back up around the mast. It then reverses its motion and repeats this sequence several times until the initial stored energy is completely dissipated. If the mast were not represented in the model, the predicted element motion would be incorrect. The model includes the out-of-plane rotation of the antenna arm and the subsequent three-dimensional motion of the complete element. The stop that the element arm contacts when it reaches its final position is represented by a nonlinear rotational spring.

The simulation was started when the element was fully unwrapped and was positioned tangential to the ring to which its root was attached. It was assumed that at this point in time the element was perfectly straight and, therefore, all of its original stored strain energy had been converted to rotational kinetic energy of the element. It is also at this position where the motion of the arm about two axes starts. It rotates about the axis of the mast and also starts to swing the element 20 degrees from the perpendicular to the mast.

With the large motion, rigid contact surface representing the mast, and the nonlinear spring representing the stop, the FE model is nonlinear and requires small time steps to

run through the deployment simulation. Several thousand time steps in the millisecond range are needed to simulate a few cycles of motion during the deployment sequence.

Predicted Stresses

Because of unknowns concerning the initial energy (velocity) of the antenna element at the start of the simulation, a parameter study was performed to determine how the stress in the element varies with the initial conditions. Figure 4 shows how the stress changes in the root of the element as the initial energy decreases. This presentation of the stresses is also useful for considering antenna response at later times. The nonlinear model is too costly to run for a full simulation, so the lower energy states were analyzed by modeling conditions as energy is gradually dissipated during the course of deployment. When the normalized stress is unity, the predicted stress in the element is at the yield stress for the titanium element. Therefore, when the two components of stress are combined, the element would deform plastically.

The results depicted in Figure 4 are not intuitive in that, for the component of stress perpendicular to the satellite (mast) axis, the stress is actually higher for a lower energy state. The stress is approximately 10 percent higher for a 75 percent energy level than for the full energy level. This can be thought of as the cyclic stress in this direction increasing during deployment for a few cycles of element motion and then gradually decreasing after that. This shows that the stress decreases in the element as the energy decreases. However, for the optimum case, the energy should be less than about 60 percent of the initial value.

Testing the response of the elements to determine whether they would permanently deform during deployment is difficult because of the effect of gravity. For vertical deployment where the antenna elements end up sloping downward, the effect of gravity subtracts from the bending stress. If the deployment is performed with the antenna in the opposite orientation, the effect of gravity adds to the stress and the elements would deform plastically.

Predicted Antenna Motion

The same parameter study discussed in the previous section predicted the antenna motion summarized in Figure 5. Here it can be seen that antenna element tip displacement toward the satellite initially increases with lower energy levels and then begins to decrease after 25 percent of the energy is dissipated. Motion away from the satellite increases as energy dissipates. Keep in mind, however, that the final tip location is approximately 0.84 m from the root location because of the 20-degree angle of the element relative to the mast.

The maximum motion toward the satellite exceeds the distance between the element and the satellite so the problem of the element tip contacting the satellite during deployment is a possibility. To illustrate this problem, Figure 6 shows the predicted position of the antenna at one point during its deployment without any energy dissipating features present. Note that the antenna element would "brush" the base of the satellite and could damage solar cells located near the base of the satellite.

Minimizing Stresses and Displacements

To dissipate the released energy and thus minimize stress and motion, several hollow cylindrical beads were placed on each element. When the element unfurls, the beads slide outward and, as they accelerate, a portion of the element's rotational kinetic energy transfers to radial outward motion of the beads. Kinetic energy in the beads in the radial direction couples inefficiently into deformation of the element and decreases energy available to cause out-of-plane motion. Several short beads were required to allow the antenna element to wrap around the canister cylinder during the stowing operation.

The outward (radial) motion of the beads is arrested by a stop at the end of the element. Additional energy losses occur when the beads impact each other and the stop. There will also be some losses from friction between the beads and the antenna element.

Modeling Bead Motion

The effects of the bead motion were determined by using a simple model of a rigid rod (the element) with a sliding mass attached (the beads). For this model all of the beads on a single element were assumed to be contained within a single mass and friction was neglected. The coupled equations of motion for the system are

$$\ddot{r}(t) - \dot{\theta}^2(t)r(t) = 0 \tag{2}$$

$$[I_R + m_B r^2(t)]\ddot{\theta}(t) + 2\, m_B r(t)\dot{r}(t)\dot{\theta}(t) = 0 \tag{3}$$

where r(t) is the radial outward motion of the bead(s) and $\dot{\theta}(t)$ is the rotational motion of the rigid rod (element). The mass of the bead(s) is m_B and the rotary inertia of the element about its base is I_R. For the remainder of this discussion the term "bead" is synonymous with the term "beads."

Some interesting features of these equations can be noticed. First, there is a damping term associated with the rotational motion and this is the product of the radial location of the bead, the radial velocity of the bead, and the mass of the bead. Second, if the initial location of the bead is too near the root of the element, it will accelerate slowly outward so that little energy transfers before the maximum stresses are experienced. Therefore, an initial location should be found that will maximize r(t) and dr(t)/dt before the element arm contacts the stop.

The equations are coupled and nonlinear and therefore have been solved numerically using the Mathematica software (ref. 3). The numerical solution is valid until the bead reaches the end of the element. Several different bead masses were considered for the study. These masses were equal to 1.0, 0.5, and 0.25 of the total antenna element mass. After considering the energy transferred to radial motion of the bead for each case, along with other factors such as the number of beads that could be conveniently packaged in the stowed antenna, the lowest mass of beads (0.25 of mass of element)

was chosen. Doubling the mass of the beads decreased the energy by about 50 percent more.

The initial radial position on the element was set at 0.26 of the element length outward from the root. This position caused the bead to reach the end of the element at the same time the element arm contacts the stop. The required time for this motion is 0.238 second. Figure 7 shows the rotational velocity of the element as a function of time up to 0.238 second and Figure 8 shows the fraction of system energy that is converted to radial bead motion as a function of time. At 0.238 second, approximately 43 percent of the energy resides in radial motion of the bead. This amount exceeds the target of 40 percent discussed previously.

The ABAQUS FE model was modified in an attempt to simulate the bead motion during deployment. Because of the highly nonlinear nature of the bead sliding along the element, the simulation became too time consuming to simulate the motion until the bead reached the end of the element. However, the 70 ms of motion that was simulated verified the motion predicted by the simple rigid rod model discussed here.

ABAQUS was also used to determine the approximate response of the element with the mass of the bead located at its end after 43 percent of the energy had been dissipated. Results of this analysis showed that the maximum expected out-of-plane displacement of the tip of the element decreased from 1.14 m toward the satellite without the beads to less than 0.73 m with the beads present, which is an acceptable amount of motion.

Reusable Release Mechanism

This mechanism releases the FORTÉ mast on command from the ground and performs the same function as a pyrotechnic cutter for less cost, with less shock, and without teardown and replacement after test. It uses a Heat Operated Paraffin (HOP) actuator*** rated at 222 N (50 lbf) push force for 3000 cycles for a stroke of 12.7 mm (0.5 in). The HOP actuator contains a paraffin that expands as it melts, and this is used to squeeze a stainless steel push rod out of a rubber boot. The actuator drive capacity is 356 N (50 lbf), however, with a safety factor of 3 applied, the maximum allowed release force is 74 N (16.7 lbf). The HOP is activated by running 28 V DC through redundant heaters at 10 W for approximately 60 seconds.

The preload that the actuator releases is 4400 N (1000 lbf). The ratio between the stowed and the release load is thus 60:1. A direct link system with a friction coefficient of 0.1 would require 444 N (100 lbf) to release this load, so a device with low friction or a long lever arm was needed, or a combination of these.

The final design uses a single roller to reduce friction as shown in Figure 9. In combination with this is a lever and drag link to maximize the release force and minimize the load on the roller. The contact surfaces are made of titanium with a yield strength of 1103 MPa (160 ksi) ultimate tensile strength, and a modulus of elasticity of 110000 MPa (16 million lb/in^2). High strength and a low modulus combine to maximize the contact stress capacity for a given weight and size.

***HOP actuator manufactured by STARSYS Research Corporation, Boulder, CO.

The titanium is coated with electroless nickel to prevent galling. It has five moving parts not including the HOP actuator which is a purchased part. The force required to release the 4400 N load is approximately 31 N (7 lbf). The HOP actuator capacity has been rated upwards by test to 80 lbf, so the factor of safety on release for the completed design exceeds 11. The springs that are critical to operation are redundant. These springs prevent premature release during vibration and reset the HOP actuator after operation. The tie rod is attached to the mechanism by pushing the tie rod member inside the mechanism from the bottom and then pulling back it out which locks the tie rod into the ready position. Proper setup can be verified visually. The unit also has a safety pin that prevents premature operation.

This device has passed all qualification tests including vibration and thermal vacuum, and is set to be launched in 1995 with the FORTÉ spacecraft.

Conclusions

The FORTÉ antenna is a device conceived for a unique application. It combines a proven Astromast™ deployer with an antenna configuration developed by LANL/SNL. The antenna has passed all tests and the next step is integration into the FORTÉ spacecraft for launch in 1995.

References

1. Timoshenko, "Strength of Materials," 3rd Edition, D. Van Nostrand and Company, pp. 54-56.
2. Hibbitt, Karlsson, and Sorensen, Inc., ABAQUS Users' Manual Version 5.2, Providence, Rhode Island (1992).
3. Wolfram Research, Inc. Mathematica Version 2, Champaign, Illinois (1992).

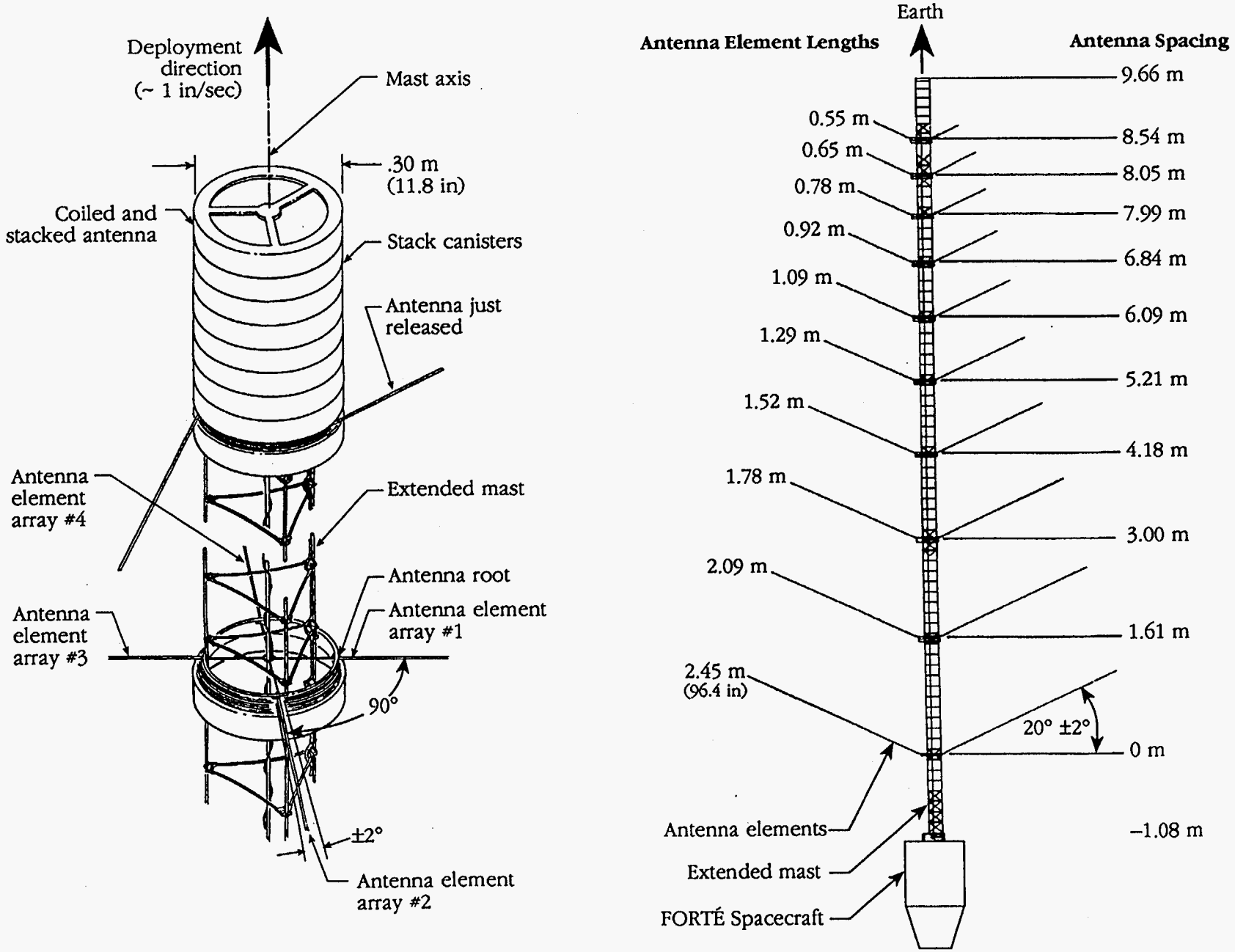

Figure 1. FORTÉ Antenna Deployment Schematic and Configuration After Fully Extended.

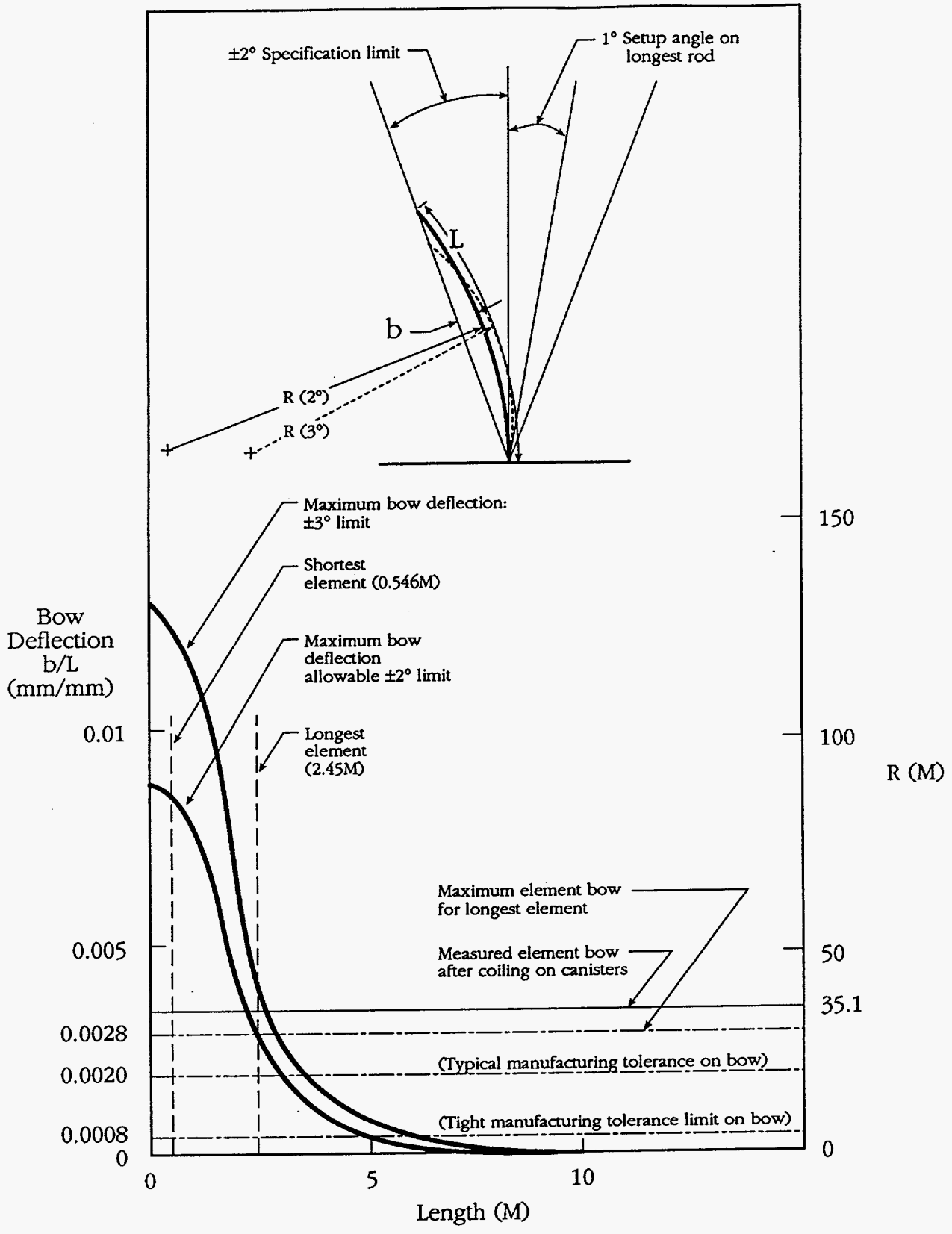

Figure 2. Required Straightness of Antenna Element as Length Increases and Setup Angle.

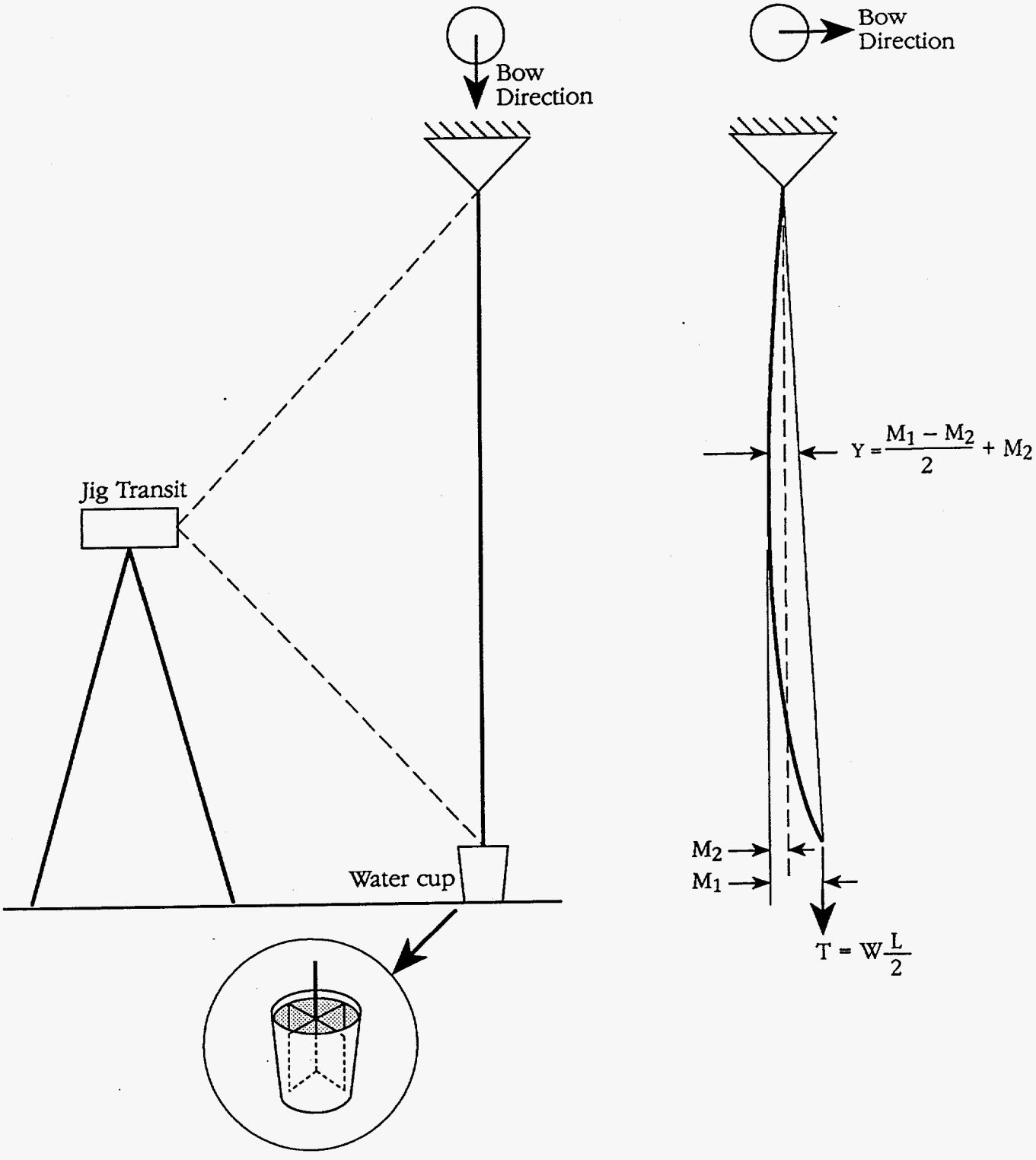

Figure 3. Measuring Bow Deflection of a Suspended Rod.

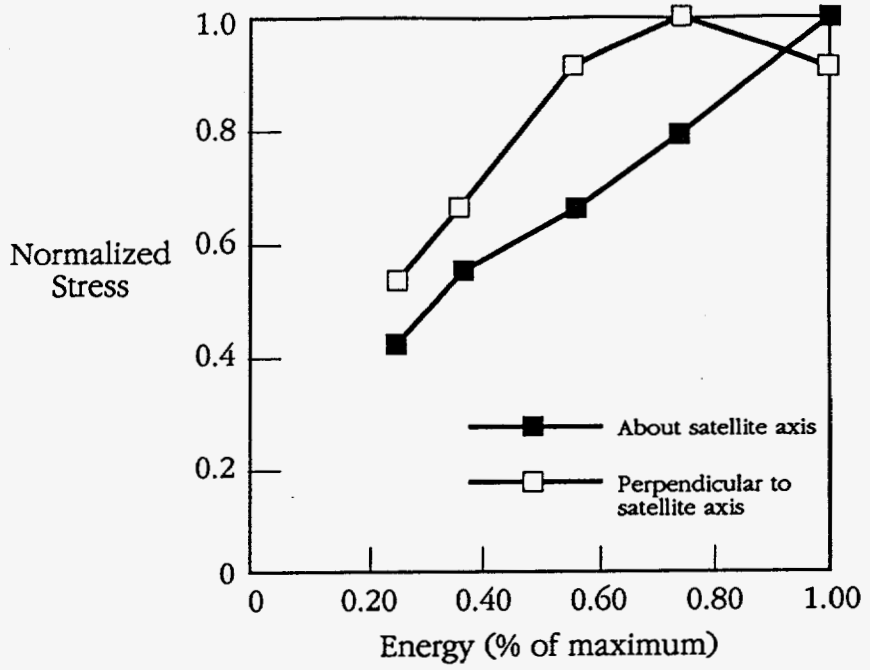

Figure 4. Maximum Bending Stress at the Root of the Antenna Element as a Function of Initial Kinetic Energy.

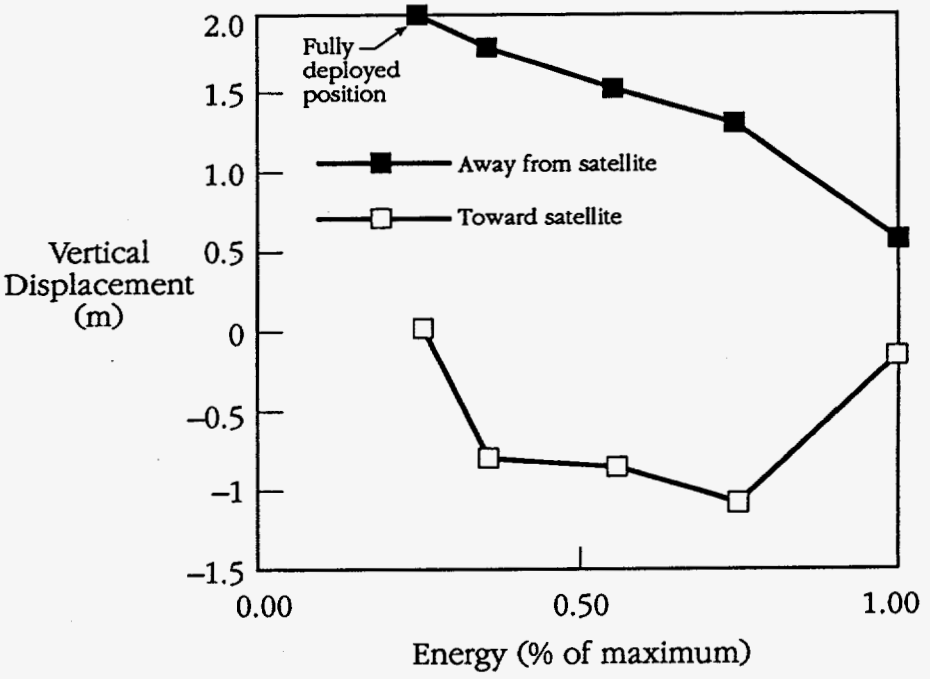

Figure 5. Maximum Vertical Displacement of Antenna Tip as a Function of Initial Kinetic Energy.

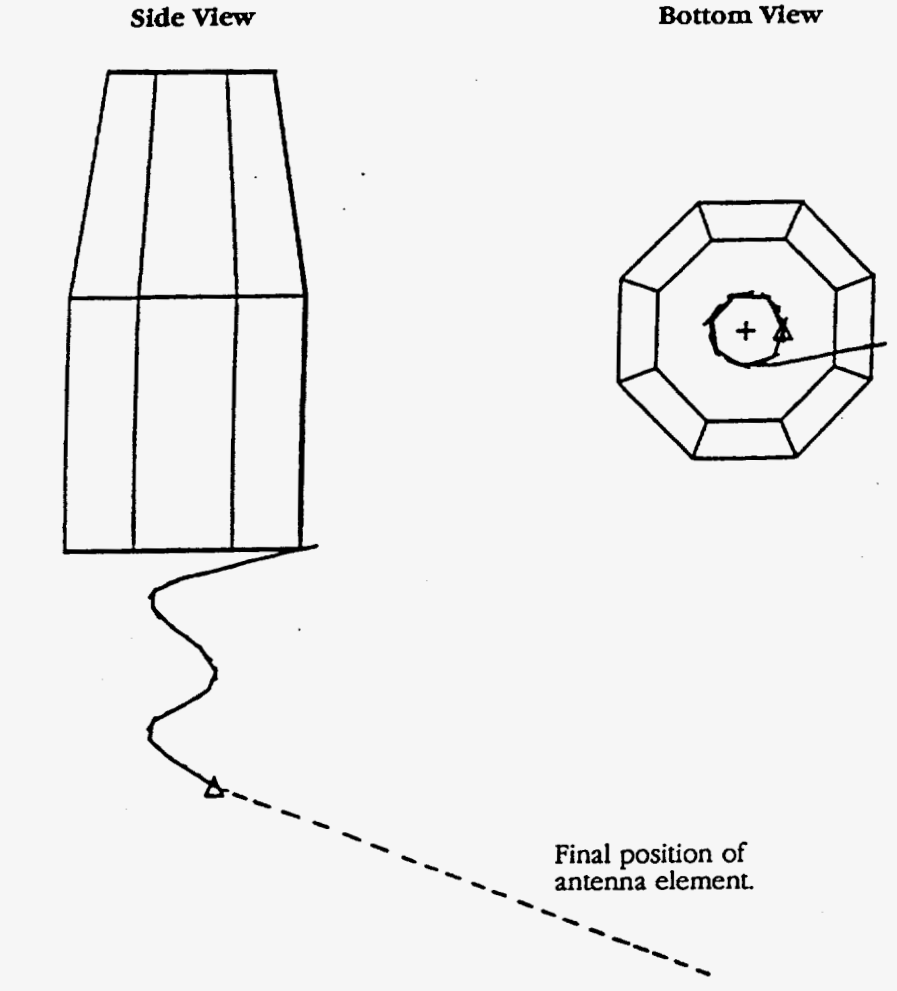

Element is shown contacting the bottom corner of the satellite.

Figure 6. Position of One Antenna Element at One Point of Time During Deployment Without any Energy Dissipation Features Implemented.

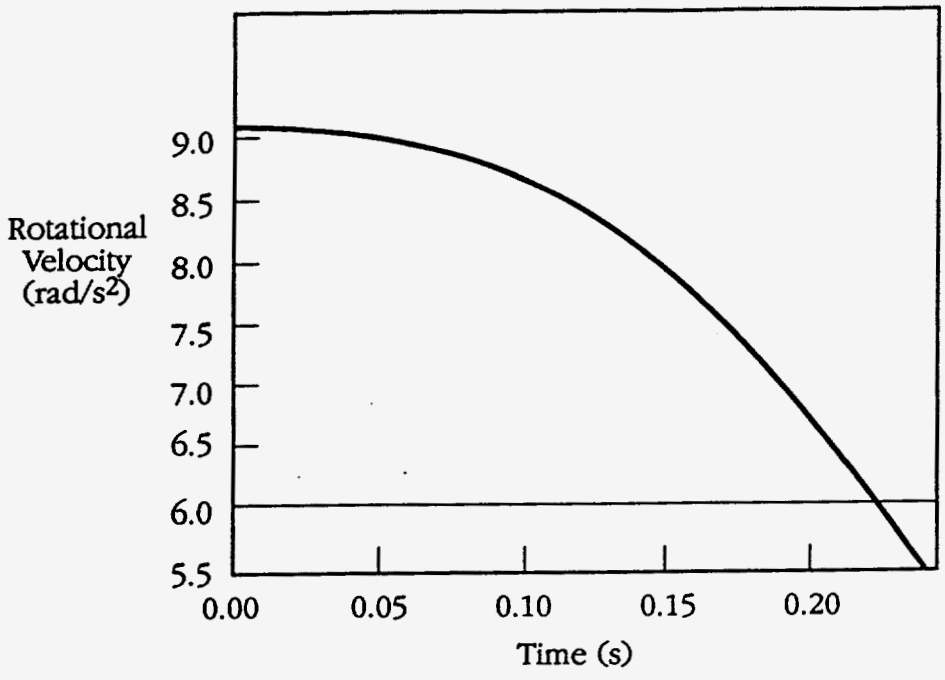

Figure 7. Rotational Velocity of Rigid Rod as a Function of Time.

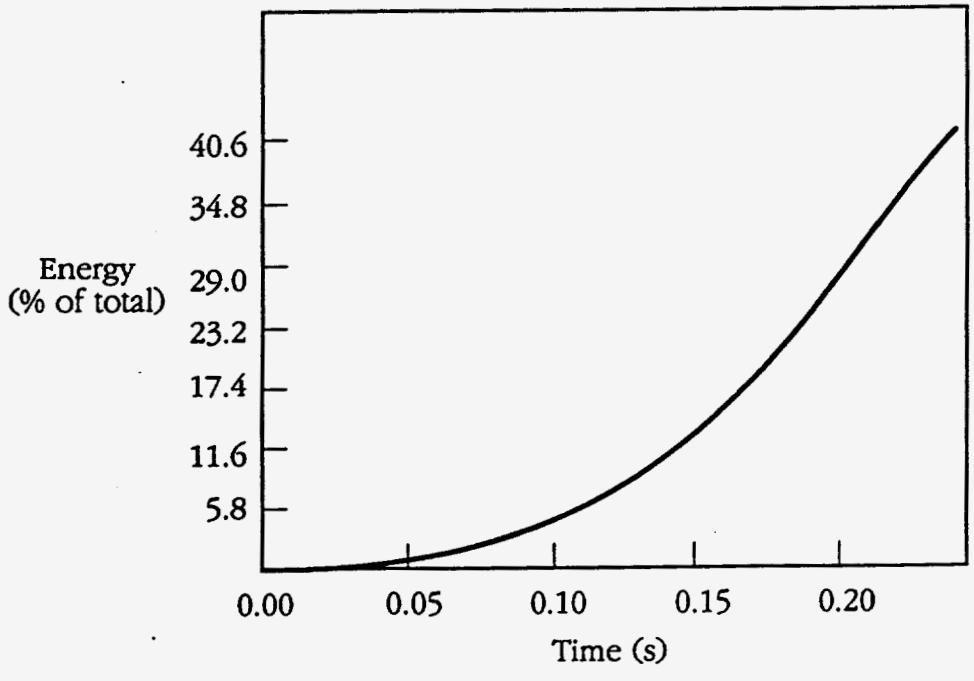

Figure 8. Percent of Total Energy Residing in Radial Motion of Bead as a Function of Time.

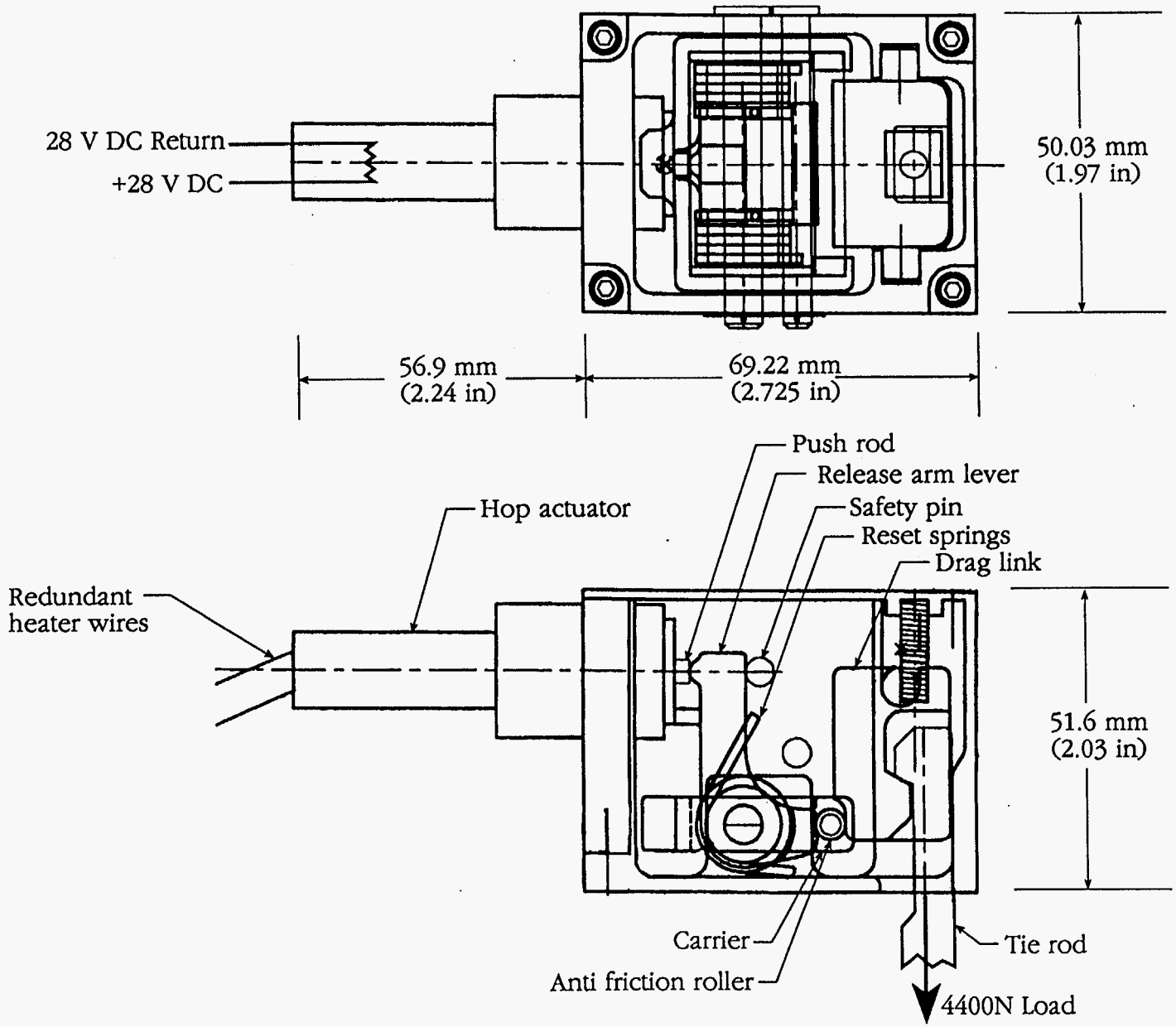

Figure 9. Schematic of the Reusable Release Mechanism.